CERN Summer Student Project Report:

Study of Trigger Efficiencies for di-Higgs Production in the ATLAS Detector using Run-3 and Run-4 Data

Name: Huda Muhydin Al Muwaness

Supervisors: Lukas Pfaffenbichler,
Tancredi Carli

October 3, 2025

Contents

Abstract

This project evaluates the performance of the ATLAS Level-1 calorimeter for di-Higgs production ($HH \to b\bar{b}b\bar{b}$ and $b\bar{b}\tau^+\tau^-$), a key process for measuring the Higgs self-coupling. The efficiency of the four jet multi-jet trigger was studied as a function of the di-Higgs mass and the transverse momentum of the fourth jet using simulated events under Run 3 and Run 4 conditions. Trigger emulation was performed, and events were filtered using jet triggers. While the efficiency is higher in the Run 4 scenario, this increase is primarily driven by a greater abundance of low-p_T jets from pile-up. This result indicates that robust pile-up suppression techniques will be essential for effective multi-jet triggering in further upgrades of the ATLAS detector.

1 Introduction

The ATLAS experiment [1] is one of the two general-purpose detectors at the Large Hadron Collider (LHC) at CERN, operating at a center-of-mass energy of $\sqrt{s}$ = 13 TeV. The ATLAS Collaboration is a large international scientific collaboration on particle physics research.

Since the discovery of the Higgs boson in 2012, the next scientific goal has been to measure its properties, one of which is the measurement of the **Higgs boson self-coupling**. This can give better insight into the electroweak symmetry-breaking mechanism. The Higgs boson self-coupling can only be measured directly by studying the production of pairs of Higgs bosons (HH).

However, this task is particularly challenging because the Higgs-boson-pair production in the Standard Model is a factor of a thousand less likely than for the production of a single Higgs boson. Moreover, the signal-to-background ratio is quite small.

One of the main limitations is the level-1 trigger system, which selects a small fraction of potentially interesting events from the enormous LHC collision rate. In Run 2, and continuing into Run 3, the hardware-based Level-1 trigger struggled with low-p_T, multi-object signatures typical of Higgs pair decays, leading to reduced efficiency. With the upcoming **Run 4** at the High-Luminosity LHC (HL-LHC), major trigger upgrades are planned to cope with extreme pile-up conditions while maintaining sensitivity to rare processes such as di-Higgs production.

1.1 Di-Higgs production and Higgs Self-Coupling

The HH production allows for a direct measurement of the Higgs self-coupling (λ), which gives information about the Higgs potential and the electroweak symmetry breaking mechanism.

As illustrated in Fig. 1, there are two main contributions: the **"box" diagram**, where two initial state gluons interact via a virtual top-quark loop to produce two Higgs bosons directly, and the **"triangle" diagram**, where the top loop produces a single virtual Higgs that subsequently decays into a Higgs pair through the Higgs self-coupling term $\lambda_3 \nu h^3$, which arises from the Higgs potential after electroweak symmetry breaking and corresponds to the triple Higgs self-interaction.

Here, h denotes the physical Higgs field, so the factor h^3 represents a vertex where three Higgs bosons interact. The parameter $v \approx 246\,\text{GeV}$ is the Higgs

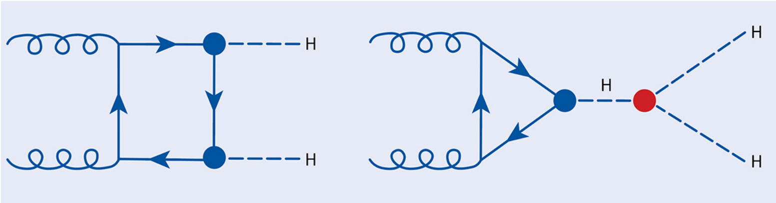

Figure 1: Examples of Feynman diagrams that describe the production of a pair of Higgs bosons at the LHC. [2]

vacuum expectation value, which sets the electroweak scale, while λ_3 is the dimensionless coupling constant that controls the strength of this cubic interaction. Physically, this interaction allows a single Higgs boson to split into two, entering directly into the "triangle" diagram of Higgs boson pair production.

One of the main characteristics of the Higgs boson is that its coupling is proportional to the mass of the particle. Therefore, the Higgs boson couples to particles in proportion to their mass. Since the top quark is by far the heaviest known elementary particle, its Yukawa coupling to the Higgs is the strongest. This makes the top-quark loop the dominant mediator in gluon–gluon fusion processes, including Higgs boson pair production.

The interplay between these diagrams is crucial as their amplitudes interfere destructively in the Standard Model, leading to a strongly suppressed production cross section [3]. Both diagrams add up at the quantum amplitude level, and destructively interfere. As a consequence, the SM HH production cross section is tiny at only $\sigma_{HH} \simeq 33\,\text{fb}$ at $\sqrt{s} = 13\,\text{TeV}$ [4].

1.2 Di-Higgs decay channels

To access this rare process experimentally, ATLAS studies multiple Di-Higgs decay channels. The four most sensitive final states currently under study are:

- $HH \to b\bar{b}\gamma\gamma$
- $HH \to b\bar{b}\tau^+\tau^-$
- $HH \to b\bar{b}WW^*$
- $HH \to b\bar{b}b\bar{b}$

In this project, particular focus is placed on the $b\bar{b}\tau^+\tau^-$ and $b\bar{b}b\bar{b}$ channels, both of which benefit from a relatively high signal yield due to their large branching ratios. However, these channels face challenges in terms of trigger selection and background suppression, particularly due to the presence of multiple low-p_T jets and τ leptons.

1.3 The ATLAS Trigger System

In Run 3, ATLAS employs a multi-stage *trigger system* to reduce the event rate from 40 MHz to 100 kHz at the Level-1 trigger, and further down to 1 kHz at the high level trigger [5]. This system makes fast decisions on whether to keep or discard collision data based on reduced information from the detector.

A key component of this is the L1Calo *jet trigger*, which identifies collimated sprays of particles (jets) originating from high-p_T quarks or gluons. The jets reconstructed at the trigger level are optimized for speed and use reduced detector granularity, while *offline jets* are reconstructed later with the full detector information and calibration [6].

Within the ATLAS trigger hardware, information is processed in the form of *Trigger Objects (TOBs)* [7]. These TOBs represent simplified versions of physics objects (e.g. jets, electrons, muons) derived from calorimeter. Logical combinations of TOBs define **trigger bits**, which determine whether an event passes the conditions specified in the trigger menu. For example, a jet trigger bit may require at least one jet above a specified p_T threshold (e.g., $p_T > 40\,\text{GeV}$) in a specific region of the detector (e.g., $|\eta| < 2.5$)

By studying the relation between trigger-level jets, offline jets, and their efficiencies, it is possible to calibrate and optimize the trigger performance. This ensures that ATLAS remains sensitive to processes of interest, even under the high pile-up conditions expected at the HL-LHC.

1.4 The Level-1 Trigger System

The Level-1 (L1) trigger system is divided into a calorimeter trigger **(L1Calo)** and a muon trigger **(L1Muon)**. These systems decide if the event is selected or rejected based on pre-defined selection parameters. The total L1 output rate is limited to 100 kHz due to detector readout constraints [7].

One of the main limitations in Run 2 and Run 3 has been the performance of the L1Calo [8] system, which struggles to efficiently trigger complex, multi-object final states with noticeably low transverse momentum, such as those produced in di-Higgs events. The constraints of the hardware-based L1 system, including granularity and fixed latency, constrain the trigger thresholds to be relatively high.

To address this, major upgrades are planned as part of the ATLAS Phase-2 upgrade for the High-Luminosity LHC (HL-LHC) [9]. Pile-up is expected to be at a nominal of 140 interactions per bunch crossing and reach up to 200. This high collision density increases the probability of producing such rare events despite the added complexity it brings to their detection and analysis. The increased luminosity is expected to significantly enhance the event yield for processes like $HH \to bb\tau\tau$ and $HH \to 4b$.

The aim of this project is to evaluate the trigger efficiencies of the Phase-1 L1Calo trigger system to be consistent with the Phase-2 upgrade and investigate possible improvements. By using Di-Higgs events from Monte-Carlo simulations and applying different trigger selections, the influence of the Run-4 conditions on the trigger efficiencies is quantified. These studies are essential for optimizing analysis strategies and informing the design of future trigger configurations.

2 Methodology

The entire analysis was built using the ROOT framework's `RDataFrame` tool [10]. `RDataFrame` provides a high-level, declarative interface for efficient data analysis in particle physics.

2.1 Jet collection and Event Selection

The analysis code is implemented as a Python script that leverages `RDataFrame`'s functional-style API to define a series of transformations and actions on the input xAOD data. The initial setup involves loading necessary libraries, configuring the runtime environment for xAOD handling, and defining key analysis parameters. The following snippet shows the beginning of this setup, including the crucial choice of which jet collection to use, depending on the dataset and analysis mode:

- **AntiKt4EMPFlowJets** (`xAOD`): the standard offline jet collection in the standard ATLAS data samples.
- **AnalysisJets** (`PhysLite`): a reduced-size collection optimized for fast analysis.

```
USE_PHYS_LITE = True
if USE_PHYS_LITE:
    jet_collection = "AnalysisJets"
else:
    jet_collection = "AntiKt4EMPFlowJets"
```

The jet objects from the xAOD/PhysLite containers are transformed into `ROOT::Math::PtEtaPhiMVector` objects. This standard ROOT class provides direct access to kinematic components (.pt(), .eta(), .phi(), .mass()) and simplifies subsequent calculations, such as angular separations or invariant mass reconstruction. This transformation is performed by looping over the original container, and accessing each jet's properties:

```
d['base'] = d['base'].Define("JetVec", f"""
    ROOT::VecOps::RVec<ROOT::Math::PtEtaPhiMVector> jets;
    for (size_t i = 0; i < {jet_collection}.size(); ++i) {{
        ROOT::Math::PtEtaPhiMVector vector(
            {jet_collection}.at(i)->pt()*0.001,
            {jet_collection}.at(i)->eta(),
            {jet_collection}.at(i)->phi(),
            {jet_collection}.at(i)->m()*0.001);
        jets.emplace_back(vector);
    }}
    return jets;
""")
```

From these four-vectors, standard kinematic quantities are extracted for each jet: (`Jet_pt`, `Jet_eta`, `Jet_phi`, `Jet_m`)

2.2 Jet Selection and Event Filtering

After the jet collection has been defined, additional selections are applied to ensure the quality of the reconstructed jets used in the analysis. First, jets are required to lie in the central region of the detector by imposing the condition $|\eta| < 2.5$. This defines the *Central Jets* collection, which serves as the starting point for further selections.

```
Central_Jet = JetVec[abs(Jet_eta) < 2.5]
```

To offline jets from pile-up interactions, a Jet Vertex Tagger (JVT) discriminant is applied. Jets within $|\eta| < 2.5$ are filtered using the requirement JVT > 0.9, which defines the JVT-selected jets:

```
Jets_JVT_cut = JetVec[(abs(Jet_eta) < 2.5) && (Jet_JVT > 0.9)]
```

In addition, a timing cut is imposed to remove non-collision background and out-of-time pile-up: jets are required to have $|t| < 10$ ns, forming the Timing-selected jets:

```
Jets_Timing_cut = JetVec[(abs(Jet_eta) < 2.5) && (abs(Jet_timing) < 10)]
```

Subsequently, a combined selection is applied, requiring both the JVT and timing criteria to be satisfied, yielding the final collection of JVT+Timing-selected jets:

```
Jets_JVT_Timing_cut = JetVec[(abs(Jet_eta) < 2.5) && (abs(Jet_timing) < 10) && (Jet_JVT > 0.9)]
```

Evaluating trigger efficiencies requires filtering on either trigger bits or an emulated trigger decision. For instance, the efficiency of `L1_4jJ40p0ETA25` trigger was studied by applying the trigger decision before prescale. This trigger requires the presence of at least four central jets with transverse momentum above 40 GeV and within $|\eta| < 2.5$.

2.3 Trigger Emulation

Trigger conditions are emulated at the analysis level to reproduce the online selection. Trigger emulation mimics the formation of the trigger bit by applying the same kinematic criteria to trigger objects (TOBs), and is used to validate the trigger by comparing the trigger decision with what the decision should have been based on a selection on the trigger objects. Trigger emulation also provides a flexible way to project the impact of future upgrades, such as jet resolution and p_T thresholds.

Trigger conditions are emulated at the analysis level to reproduce the online selection. A helper function is declared, which counts the number of jets above a configurable p_{T} threshold and within a given eta range:

```
int EmulateTrigger(const ROOT::VecOps::RVec<ROOT::Math::PtEtaPhiMVector>& jets, int n_jets, double eta_low, double eta_high, double pt_thresh) {
    int count = 0;
    for (const auto& jet : jets) {
        if (jet.eta() < eta_high && jet.eta() > eta_low && jet.pt() > pt_thresh) {
            count++;
            if (count >= n_jets) return 1;
        }
    }
    return 0;
}
```

Both single-jet ($j40$) and multi-jet ($4j40$) requirements are implemented, applied to offline jets as well as to Level-1 trigger objects (TOBs).

2.4 Di-Higgs Mass Reconstruction

In this analysis, the di-Higgs invariant mass is reconstructed from truth-level Higgs bosons. First, to select the Higgs Bosons, a collection of Higgs bosons are defined by looping over the generator-level bosons in the event record. Each selected Higgs boson is stored as a four-vector of type `PtEtaPhiMVector`. This produces a vector of Higgs bosons, hereafter denoted `HiggsBosons`.

Then, to calculate the Di-Higgs invariant mass, the di-Higgs system is reconstructed by combining the four-vectors of the first two Higgs bosons in the event:

```
    d['base'] = d['base'].Define("Di_Higgs_Mass", '(HiggsBosons.at(0) + HiggsBosons.at(1)).M()')
```

Here, the two four-vectors are added according to relativistic kinematics, and the invariant mass of the combined system is calculated.

A histogram of the di-Higgs invariant mass is produced to provide a basis for studying the kinematic properties of the Higgs boson pair later on.

After applying signal trigger requirements on di-Higgs events, the di-Higgs invariant mass is plotted in another histogram.

2.5 Trigger Efficiency

To quantify the performance of the trigger selections, efficiencies were computed by dividing the signal histograms by the corresponding monitor histograms. Signal histograms represent events that pass a given trigger requirement.

For each observable under study, the efficiency is defined as

$$\epsilon(x) = \frac{N_{\text{signal}}(x)}{N_{\text{monitor}}(x)},$$

where $N_{\text{signal}}(x)$ and $N_{\text{monitor}}(x)$ are the bin contents of the signal and monitor histograms, respectively.

The division is performed bin-by-bin. A binomial error treatment (option "B" in the ROOT TH1::Divide method) is used to correctly propagate statistical uncertainties.

The calculation is implemented in a standalone Python script by retrieving the monitor and signal histograms, and dividing them to produce efficiency histograms. The script loops over predefined sets of histogram names corresponding to jet multiplicities, p_T ordering, di-Higgs mass distributions, and different event selections (e.g., central jets, JVT cuts, timing cuts).

3 Results

Following the established methodology, the results for the trigger efficiencies are presented.

3.1 Comparison of Run-3 and Run-4 Jet p_T4

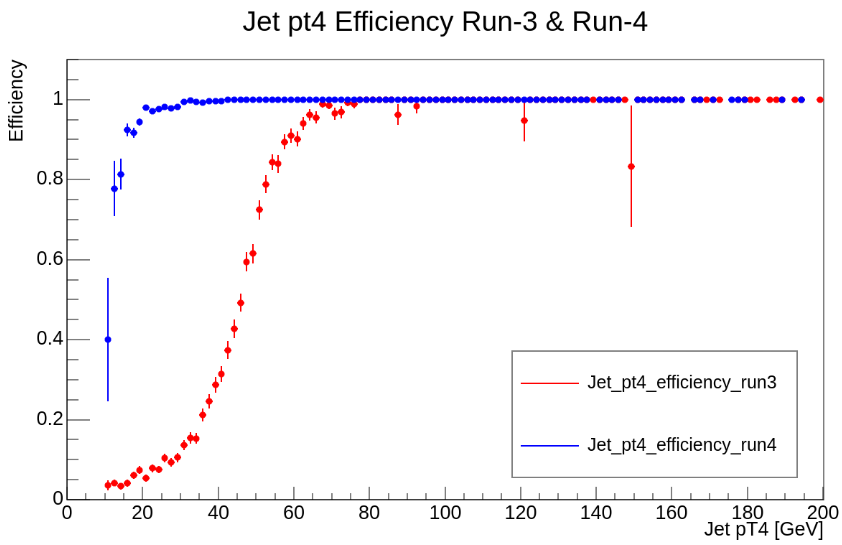

Figure 2: Multi-jet Trigger Efficiency as a function of the transverse momentum of the fourth leading jet from Run-3 (Red) and Run-4 (Blue)

Figure 2 presents a comparison of the trigger efficiency for the L1_4jJ40p0ETA25 trigger between Run-3 and Run-4 conditions for di-Higgs events. Efficiency is plotted as a function of the transverse momentum of the fourth leading jet (p_{T4}).

The Run-3 simulation curve (shown in red) demonstrates the expected performance under current LHC conditions. The turn-on curve reaches a plateau of approximately 95% efficiency for jets with $p_T > 70$ GeV, with a 50% efficiency point located at roughly 50 GeV.

The Run-4 simulation curve (shown in blue) demonstrates a sharper turn-on curve and reaches a higher plateau efficiency of near 100% at a lower p_T. Most notably, the 50% efficiency point is shifted to a lower pT of approximately 25 GeV. This apparent increase in efficiency is a consequence of the high pile-up conditions in Run-4, which produce an abundance of low-p_T jets that satisfy the trigger's kinematic requirements.

3.2 Trigger Performance as a Function of Jet Kinematics

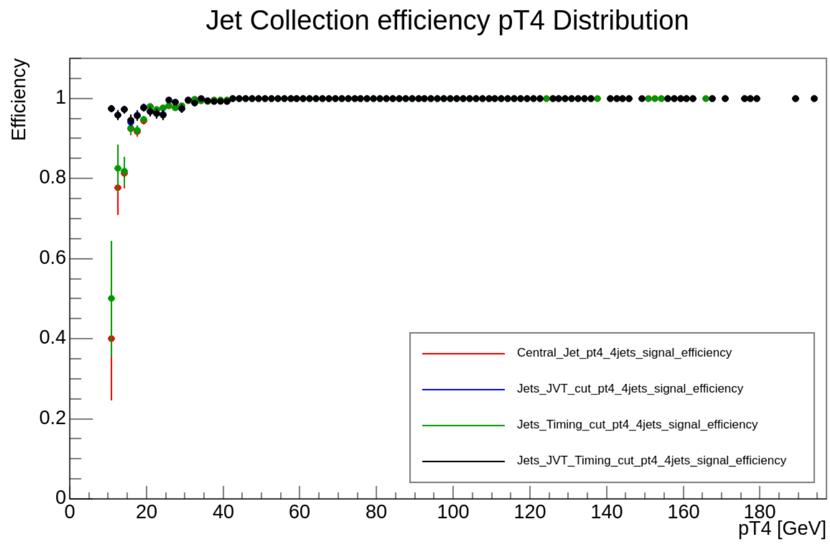

Figure 3: Multi-jet trigger efficiency with regard to the transverse momentum of the 4th jet for different jet collections.

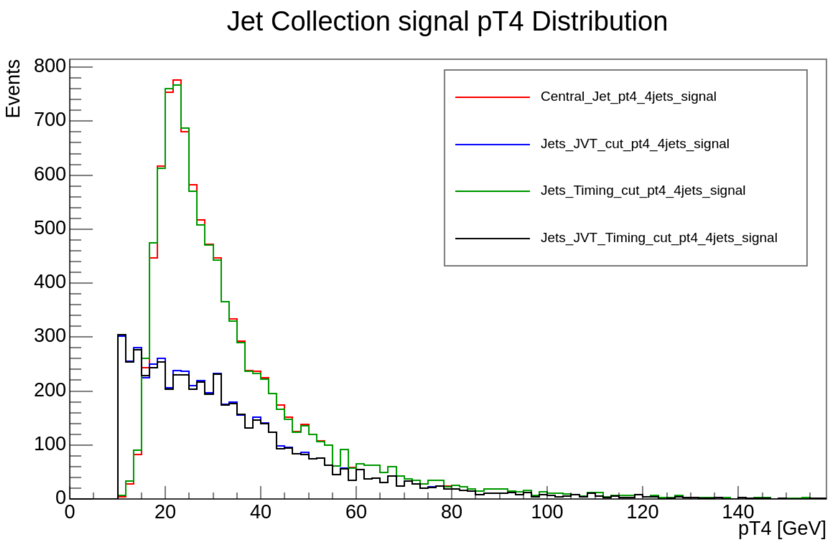

Figure 4: Distribution of p_{T4} for events passing the signal trigger.

Figure 3 shows the impact of different jet selection strategies on the trigger efficiency for the fourth-leading jet transverse momentum, p_{T4}. The offline JVT and timing cuts of the fourth leading jet greatly reduce the number of events passing the trigger. The high efficiency is a result of the high pile-up and would lead to an unsustainably high trigger rate.

Figure 4 shows that the central jet collection exhibits a broader distribution due to the presence of pile-up jets. After applying the JVT and timing requirements, the signal distribution becomes narrower and more consistent with the expected kinematics of hard-scatter jets. This illustrates the importance of handling the jets from in-time and out-of-time pile-up interactions in Run-4 correctly.

3.3 Performance as a Function of di-Higgs Mass

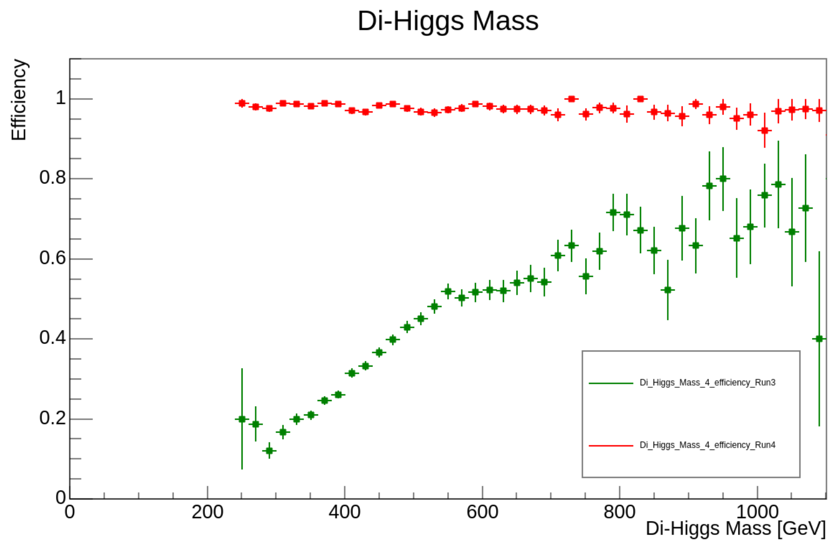

Figure 5: Trigger efficiency as a function of the di-Higgs invariant mass m_{HH} of the fourth leading jet for Run-3 (green) and Run-4 (red).

Figure 5 compares the efficiency of the `L1_4jJ40p0ETA25` trigger as a function of the di-Higgs mass of the fourth leading jet in Run-3 emulated trigger conditions with an average pileup of $\mu = 50$ (green points), and the Run-4 emulated trigger with nominal pileup of $\mu = 140$ reaching up to $\mu = 200$ (red points).

For the Run 3 case, the efficiency is strongly dependent on the di-Higgs mass. At low m_{HH} values (below about 500 GeV), the efficiency is significantly reduced. This behavior is driven by the kinematics of the Higgs decay: at lower m_{HH} the b-jets tend to have lower transverse momenta, and many of them fail to pass the relatively high trigger thresholds used in Run-3. As the di-Higgs system becomes more boosted at larger invariant masses, the jets are more energetic, and the efficiency correspondingly increases. At the highest m_{HH} values, statistical fluctuations become large due to limited event counts.

It is crucial to note that the trigger selection is identical for both the Run-3 and Run-4 emulations. Therefore, the improved performance does not stem from upgrades to the trigger logic, but rather from the higher pile-up conditions in Run-4.

This high pile-up environment results in a much larger number of soft jets within the central detector region. Consequently, it becomes statistically more likely for any given event to contain four jets that accidentally satisfy the trigger's kinematic thresholds, irrespective of whether they originate from the hard-scatter process or from pile-up. This effect artificially inflates the trigger efficiency for the Run-4 sample.

For future investigations, it will be of interest to compare triggers at the same rate for Run-3 and Run-4 pile-up conditions and new triggers need to be developed based on the Phase-2 system.

4 Conclusion

The successful operation of the ATLAS experiment during the High-Luminosity LHC era is critically dependent on an efficient trigger system. This project has investigated the performance of the Level-1 calorimeter trigger for the di-Higgs production, a process central to understanding the nature of the Higgs self-coupling.

This report demonstrates the clear differences in the trigger efficiencies for Run-3 and Run-4 conditions. With an increase in the event yield for HH $\rightarrow$ bbbb events, it is necessary to adjust the triggers in order to correctly identify the events with a true multi-jet signature. This showcases the importance of further developments for new and improved trigger techniques for the Phase-2 upgrades. This will translate to a larger event yield of triggered Di-Higgs events, substantially increasing the statistical power for this measurement.

References

[1] G. Aad et al. The ATLAS Experiment at the CERN Large Hadron Collider. *JINST*, 3:S08003, 2008.

[2] Simon Geldard. Homing in on the higgs self-interaction. *CERN Courier*, dec 2022. Accessed: 2024-05-15.

[3] ATLAS Collaboration. Search for di-Higgs production at 13 TeV and prospects for the HL-LHC. ATL-PHYS-SLIDE-2019-705, CERN Document Server, 2019. Accessed: 2025-08-20.

[4] B. Di Micco et al. Higgs boson pair production at colliders: Status and perspectives. *Rev. Phys.*, 5:100045, 2020.

[5] ATLAS Collaboration. ATLAS High-Level Trigger, Data Acquisition and Controls: Technical Design Report. Technical Report ATLAS-TDR-016, CERN, 2003.

[6] ATLAS Collaboration. Jet energy scale measurements and their systematic uncertainties in proton–proton collisions at $\sqrt{s} = 13$ TeV with the ATLAS detector. *Phys. Rev. D*, 96(7):072002, 2017.

[7] ATLAS Collaboration. Technical Design Report for the Phase-I Upgrade of the ATLAS TDAQ System. Technical report, CERN, 2013. CERN-LHCC-2013-018, ATLAS-TDR-023.

[8] M. Aaboud et al. Performance of the atlas trigger system in 2015. *Eur. Phys. J. C*, 77:317, 2017.

[9] Technical design report for the phase-ii upgrade of the atlas tdaq system. Technical Report CERN-LHCC-2017-020, CERN, 2017.

[10] Vassil Vassilev, Philippe Canal, Axel Naumann, and Danilo Russo. Root rdataframe: Easy parallel analysis with root. *EPJ Web of Conferences*, 214:06025, 2019.